PNAS
www.pnas.org

Supplementary Information for

Ice and ocean constraints on early human migrations into North America along the Pacific coast

Summer Praetorius[1*], Jay Alder[2], Alan Condron[3], Alan Mix[4], Maureen Walczak[4] Beth Caissie[1], Jon Erlandson[5]

[1]U.S. Geological Survey, Menlo Park, CA
[2]U.S. Geological Survey, Corvallis, OR
[3]Woods Hole Oceanographic Institution, Woods Hole, MA
[4]Oregon State University, Corvallis, OR
[5]University of Oregon, Eugene, OR

*Corresponding author: spraetorius@usgs.gov

This PDF file includes:

Supplemental text
Figures S1 to S8
Tables S1 to S2
Legends for Datasets S1 to S5
SI References

Other supplementary materials for this manuscript include the following:

Datasets S1 to S5

Supplemental Text

Climate change impacts on marine ecosystems

High latitude Northern Hemisphere climate was volatile during the last glacial and deglacial periods, with abrupt warming and cooling events occurring on timescales of years to decades (1). These events would have transformed landscapes, weather systems, and terrestrial and marine ecosystems, requiring relatively rapid adaptation adjustments for ecological and human communities. Here we address how changing climate conditions may have affected marine ecosystems along the Pacific Rim, and how that may have in turn, affected human migration or coastal habitability at various times.

Kelp ecosystems and sea ice environments

Kelp forests have been hypothesized to have been key for supporting human dispersal to the Americas (2,3). Expanded convoluted shorelines and shallow rocky intertidal zones in the Beringian Transitory Archipelago during the LGM would likely have been conducive to kelp ecosystems (4). The persistence of the Steller's sea cow, a ~10-ton sirenian that relied exclusively on kelp and ranged along the Pacific Coast from Japan to California and across the Bering Sea shelf, suggests that kelp habitats remained at least regionally intact throughout the Pleistocene and early Holocene. This marine mammal may have been an important species in maintaining healthy kelp ecosystem prior to its extinction (5), and an important marine resource for ancient coastal people, as it was docile, confined to shallow waters, and provided enormous quantities of meat and oil (6). Neither Steller's sea cow nor kelp forests can survive in persistent multiyear ice; ice scouring can dislodge kelp hold fasts, and excessive freshwater input and sediment loads can negatively impact growth (7). In modern Arctic environments, however, kelp can be highly productive and well adapted to seasonal sea ice and light limitation (7). Thus, kelp environments may have thrived during the glacial period throughout coastal Beringia, despite seasonal sea ice. However, local conditions were likely highly variable in space and time, and conditions in the Gulf of Alaska during the Siku ice surge events may have been particularly antagonistic for kelp growth.

Expansions of the oxygen minimum zone

The abrupt ocean warming that occurred during the Bølling-Allerød and early Holocene periods caused major changes to marine ecosystems across the North Pacific. These events were accompanied by an expansion of the oxygen minimum zone (OMZ) across the North Pacific and rapid transitions to deep-water hypoxia, with a contraction of benthic faunal diversity at intermediate depths along the Alaskan and California margins (8,9). However, it remains unclear how this event impacted upper ocean ecosystems, such as kelp forests. On the one hand, increased primary productivity during the Bølling-Allerød may have supported thriving marine ecosystems, providing energy to fuel extensive trophic webs (Fig. S8a). As is seen in the modern Bering Sea 'Green Belt' along the shelf edge where both macro and micronutrients are available from shelf mixing, high levels of primary productivity are associated with some of the most productive marine waters, supporting large stocks of fish, squid,

waterfowl, and marine mammals (10). On the other hand, high *export* productivity doesn't necessarily indicate a healthy marine ecosystem, as export efficiency can be decoupled from primary productivity and instead reflect rapid removal of organic carbon from the upper ocean, limiting its utilization for heterotrophic grazing (11). For example, diatomaceous algal blooms can have high efficiency of carbon export that can lead to a self-sedimentation effect which promotes laminated opal-rich sediments (12), like those observed during the Bølling-Allerød. In events like this, algal blooms may induce poisoning of the food chain and/or subsurface hypoxia through rapid deoxygenation of the water column as sinking organic material is respired (Fig. S8b). It remains unclear whether ocean deoxygenation at intermediate depths impacted upper ocean ecosystems during the Bølling-Allerød and early Holocene hypoxic events.

While it is unlikely that sustained hypoxia extended into shallower depths, it is possible that the vertical expansion of the OMZ led to more frequent hypoxic events, especially in upwelling areas, such as the California Current system. Even episodic events that caused detrimental effects to reliable food sources may have been an impetus to seek additional resources inland, possibly promoting movement into the hinterlands. This may in part account for inland archaeological sites that date to the Bølling period, but no coastal evidence for occupation that has been uncovered during this period. Submergence of coastal sites by postglacial sea level rise makes locating earlier deglacial coastal sites challenging, however, a few coastal areas have remained above sea level throughout the deglaciation (13,14), so additional factors affecting the timing of habitability must be assessed. For example, the Daisy Cave site on San Miguel Island (one of the Channel Islands off southern California) contains a few artifacts and charcoal from a possible hearth feature that has been dated to ~18.6 ka (15,16). Although situated several kilometers from the coast at this time, the site was available for occupation throughout the deglaciation and remains above sea level.

With Pacific Coast archaeological sites occupied prior to the Holocene, the early Holocene hypoxic event presents a possible opportunity to assess whether OMZ expansion had discernable impacts on nearshore coastal ecosystems. A possible multi-centennial hiatus in the Channel Island occupation between ~11.1-10.7 ka (17) is similar in timing to the early Holocene hypoxic event (8,18,19), suggesting a possible connection between hypoxia and a temporary abandonment of the Channel Islands. Confirming such connections will require greater precision in linking terrestrial and marine age models, as well as additional proxy evidence for changes in species composition in response to changing climate conditions.

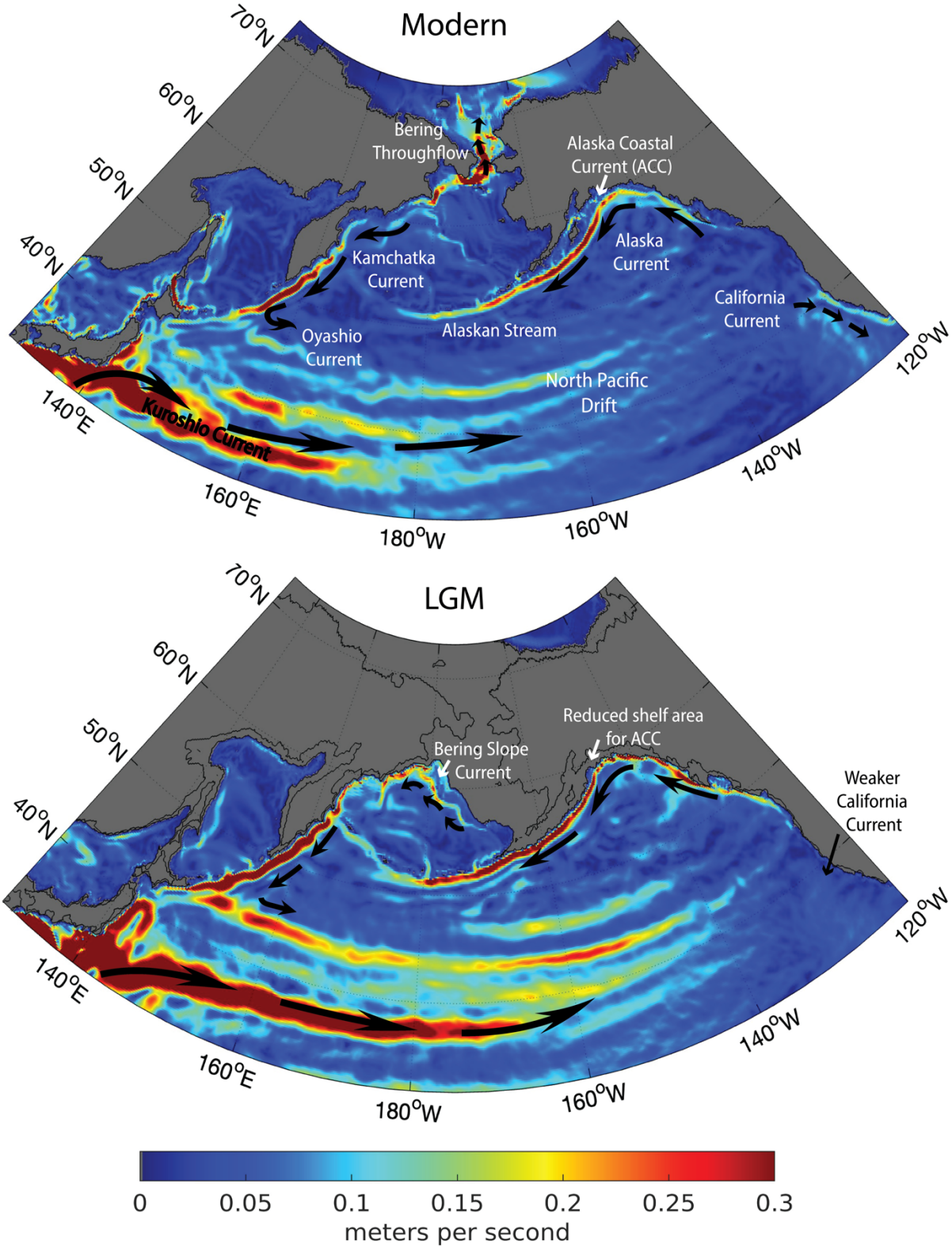

Figure S1. Simulations of ocean currents in the North Pacific during glacial and interglacial periods. Mean annual surface ocean velocity (m/s) for the modern climate state (top) and the last glacial maximum (bottom), showing a strengthening of most currents during the LGM, including the Kuroshio, Oyashio, Kamchatka, Bering Slope, and Alaska Current systems. Boundary currents flow in a cyclonic (anticlockwise) direction. The California Current is the only major current that shows a weakening during glacial conditions relative to the modern period.

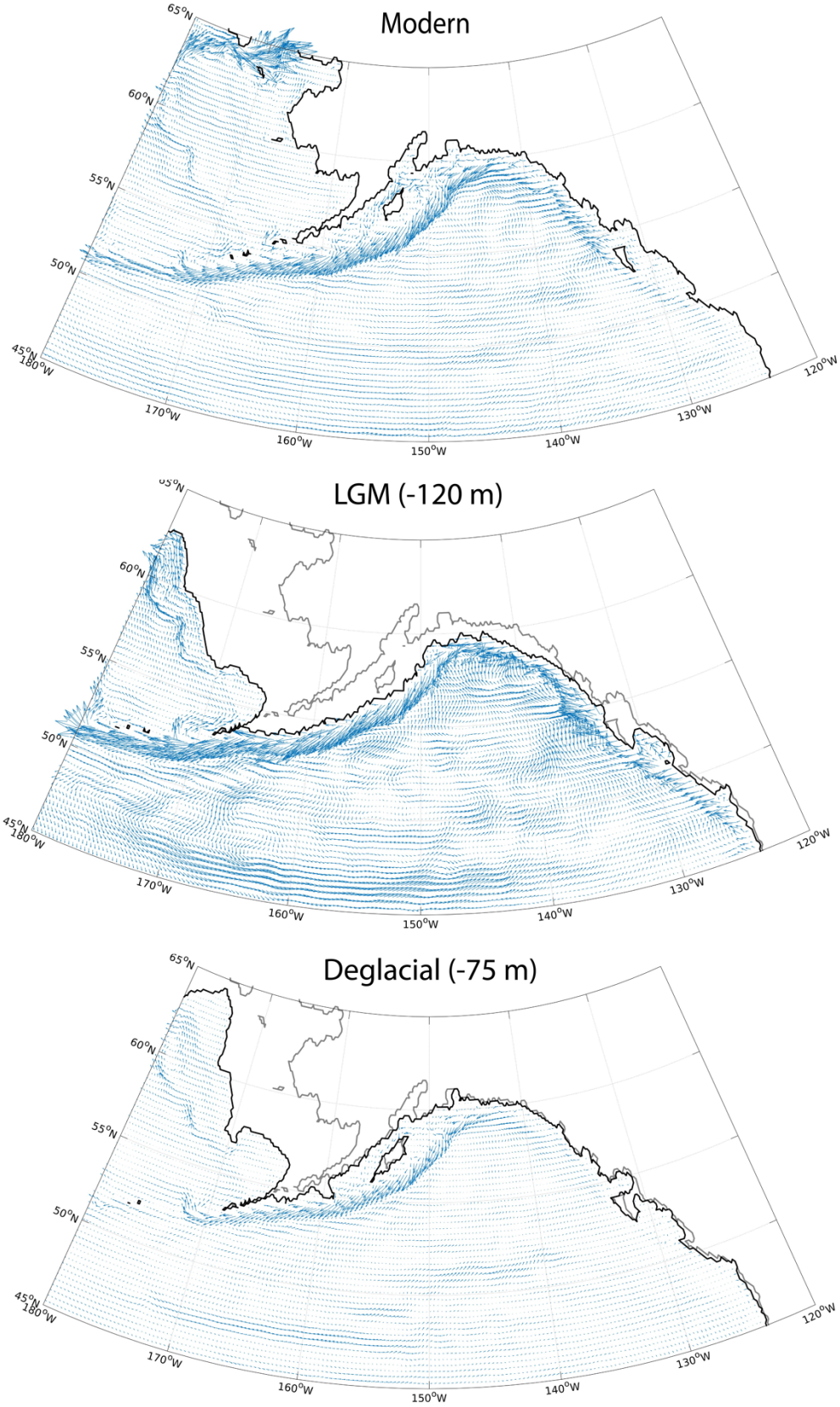

Figure S2. Ocean current vectors for the Northeast Pacific for various climate states and sea levels.

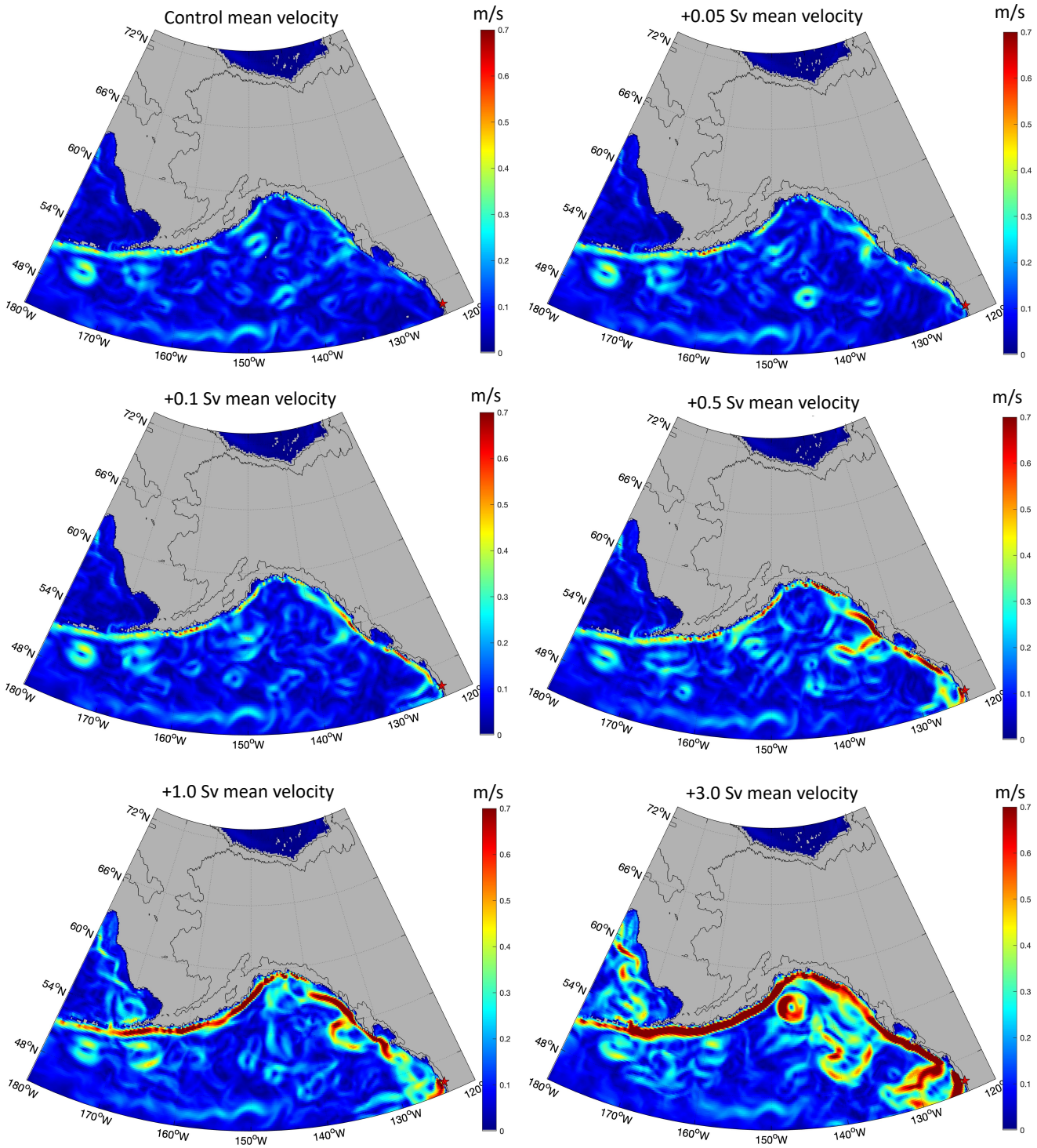

Figure S3. Mean current velocity (m/s) in glacial simulations with varying freshwater fluxes (averaged from July-Dec). Note the difference in scale shown here (0-0.7 m/s) relative to the scale shown in Fig. 2 (0-0.3 m/s) to accommodate the larger velocities associated with the high freshwater fluxes.

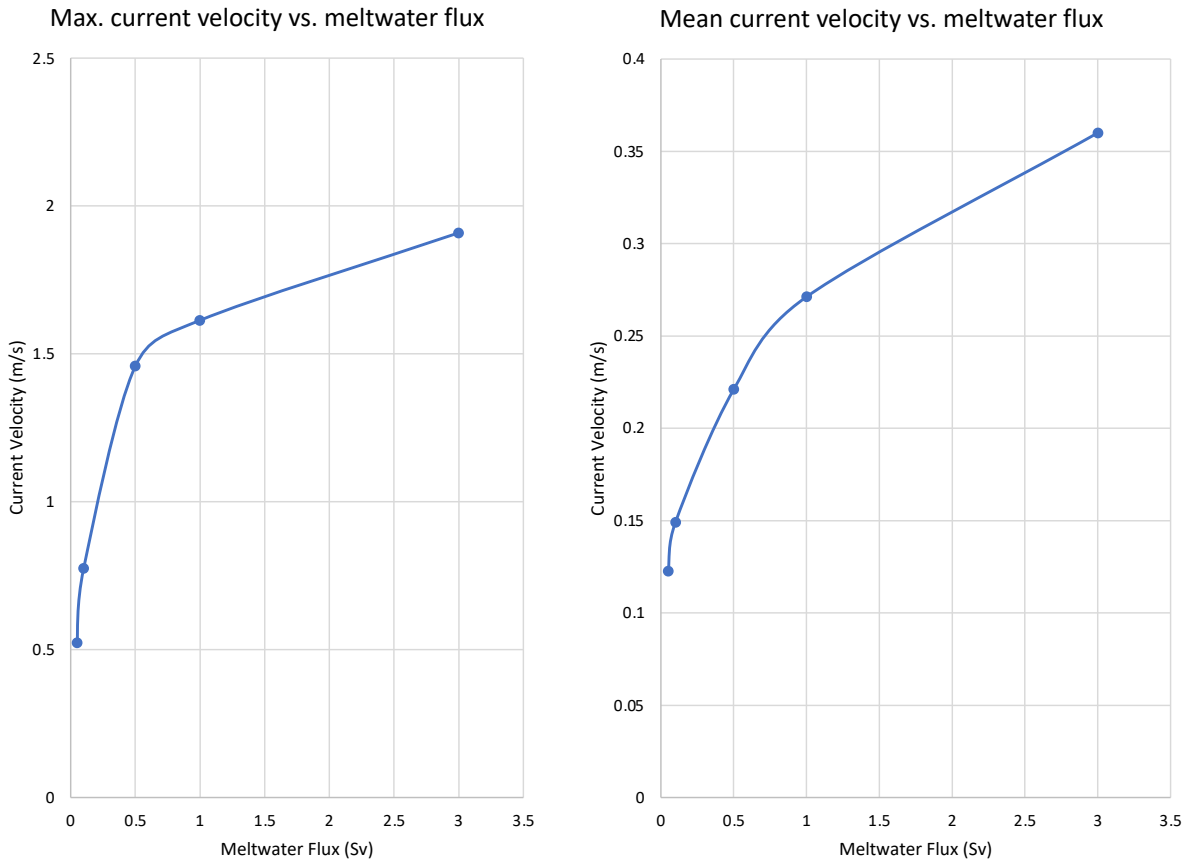

Figure S4. Maximum and mean current velocity for various meltwater fluxes shown in Figure S3.

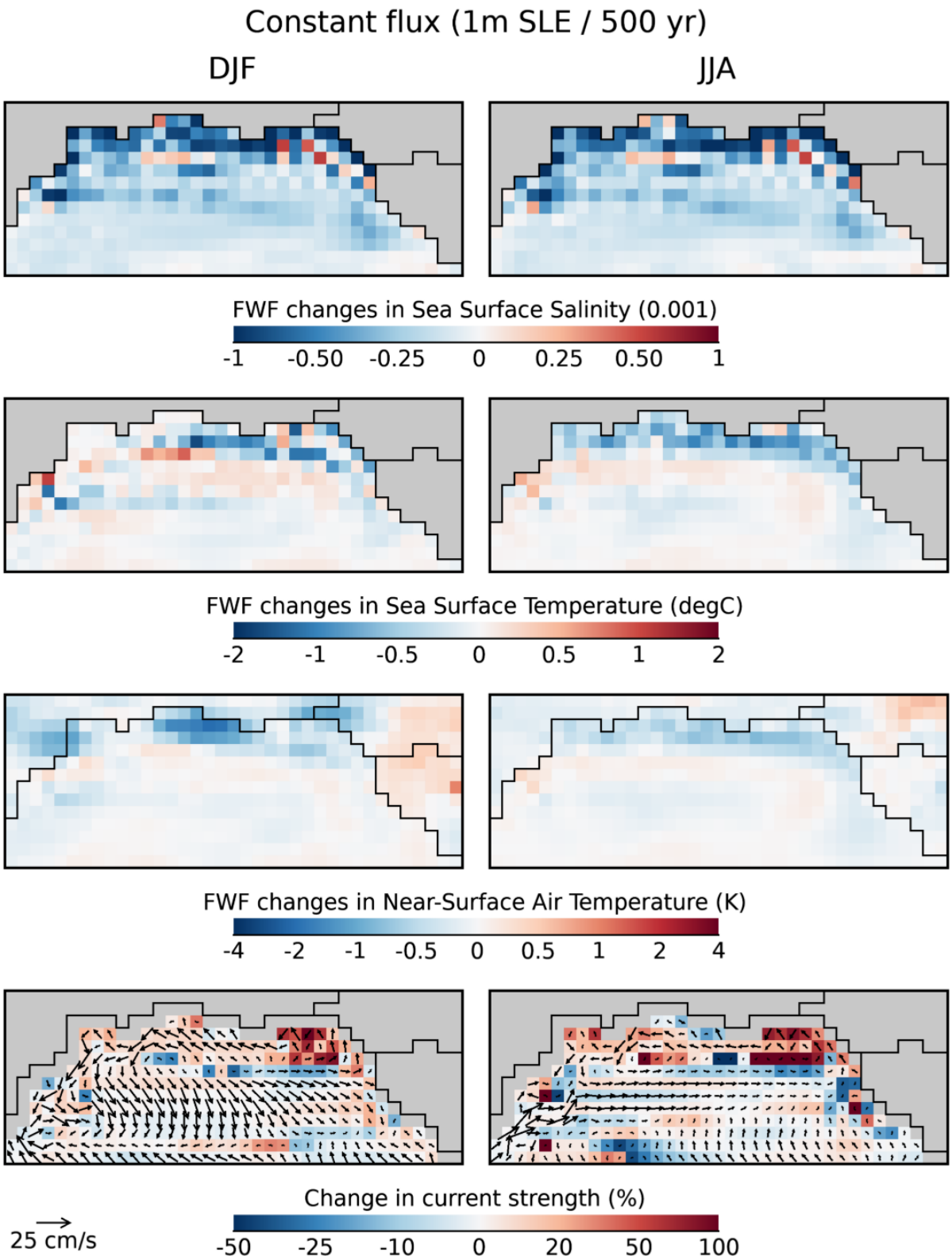

Figure S5. Changes in Winter (DJF) and Summer (JJA) surface salinity, sea surface temperature, surface air temperature, and current strength for the 1m sea level equivalent (SLE) / 500 yr freshwater flux (FWF) experiment minus control. Change in current strength (lower panel) is shown as percent change with the directional vectors overplotted from the control simulation.

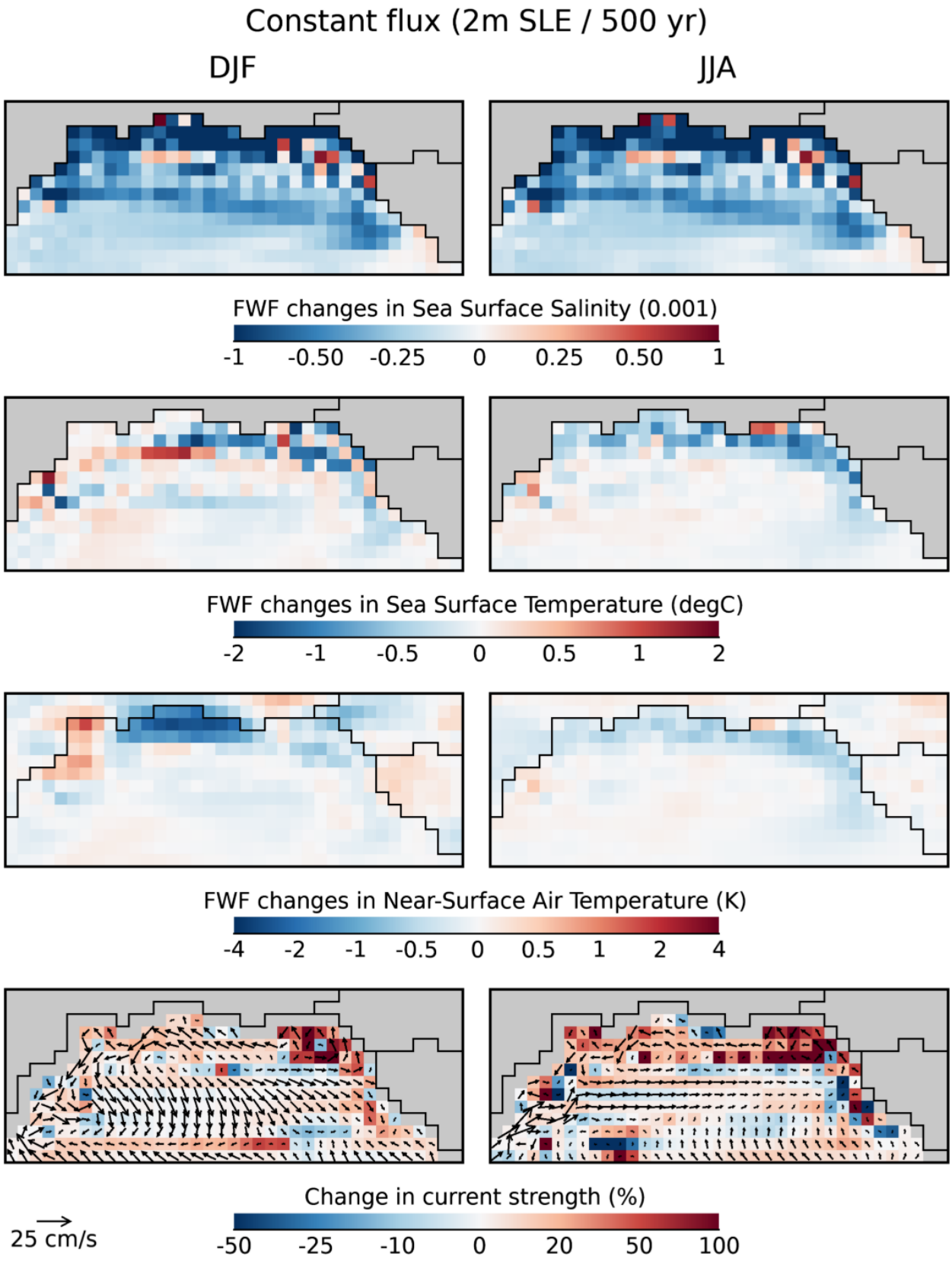

Figure S6. Same as Figure S5 for the 2m sea level equivalent / 500 yr experiment.

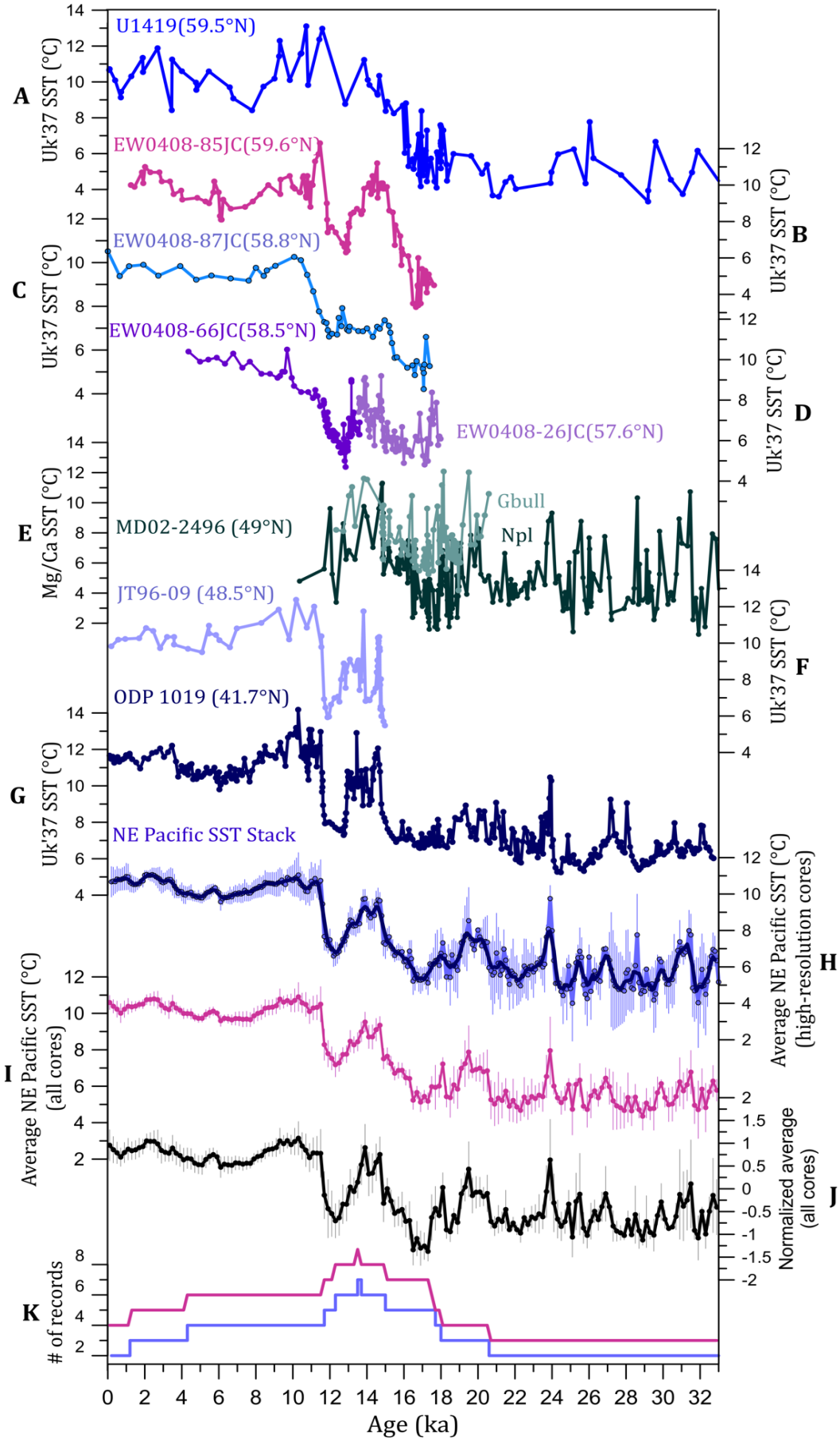
U1419(59.5°N)
EW0408-85JC(59.6°N)
EW0408-87JC(58.8°N)
EW0408-66JC(58.5°N)
EW0408-26JC(57.6°N)
MD02-2496 (49°N)
Gbull
Npl
JT96-09 (48.5°N)
ODP 1019 (41.7°N)
NE Pacific SST Stack
A
B
C
D
E
F
G
H
I
J
K
Uk'37 SST (°C)
Mg/Ca SST (°C)
Average NE Pacific SST (°C) (all cores)
Average NE Pacific SST (°C) (high-resolution cores)
Normalized average (all cores)
# of records
Age (ka)

Fig. S7. Reconstructed SST records from the Northeast Pacific margin (A-G) that contribute to the stacked average records (H-J). A) $U_{37}^{K'}$ record from U1419 (20); **B)** $U_{37}^{K'}$ record from EW0408-85JC (8), **C)** $U_{37}^{K'}$ record from EW0408-87JC (21); **D)** $U_{37}^{K'}$ record from EW0408-66JC & EW0408-26JC (22); **E)** Mg/Ca-based SST reconstruction from MD02-2496 on *Globigerina bulloides* (Gbull; light green) and *Neogloboquadrina pachyderma* (Npl; dark green) (23); **F)** $U_{37}^{K'}$ record from JT96-09 (24); **G)** $U_{37}^{K'}$ record from ODP 1019 (25,26, age/depth model modified by ref. 21); **H)** Average stack using the high-resolution records (~100-yr average or greater); **I)** Average stack using all records (on a 200 yr timestep); **J)** Normalized average using all cores; **K)** Number of records contributing to the high-resolution stack (blue) and the all-core and normalized stacks (pink). Error bars on the stacked records reflect the standard error of the mean.

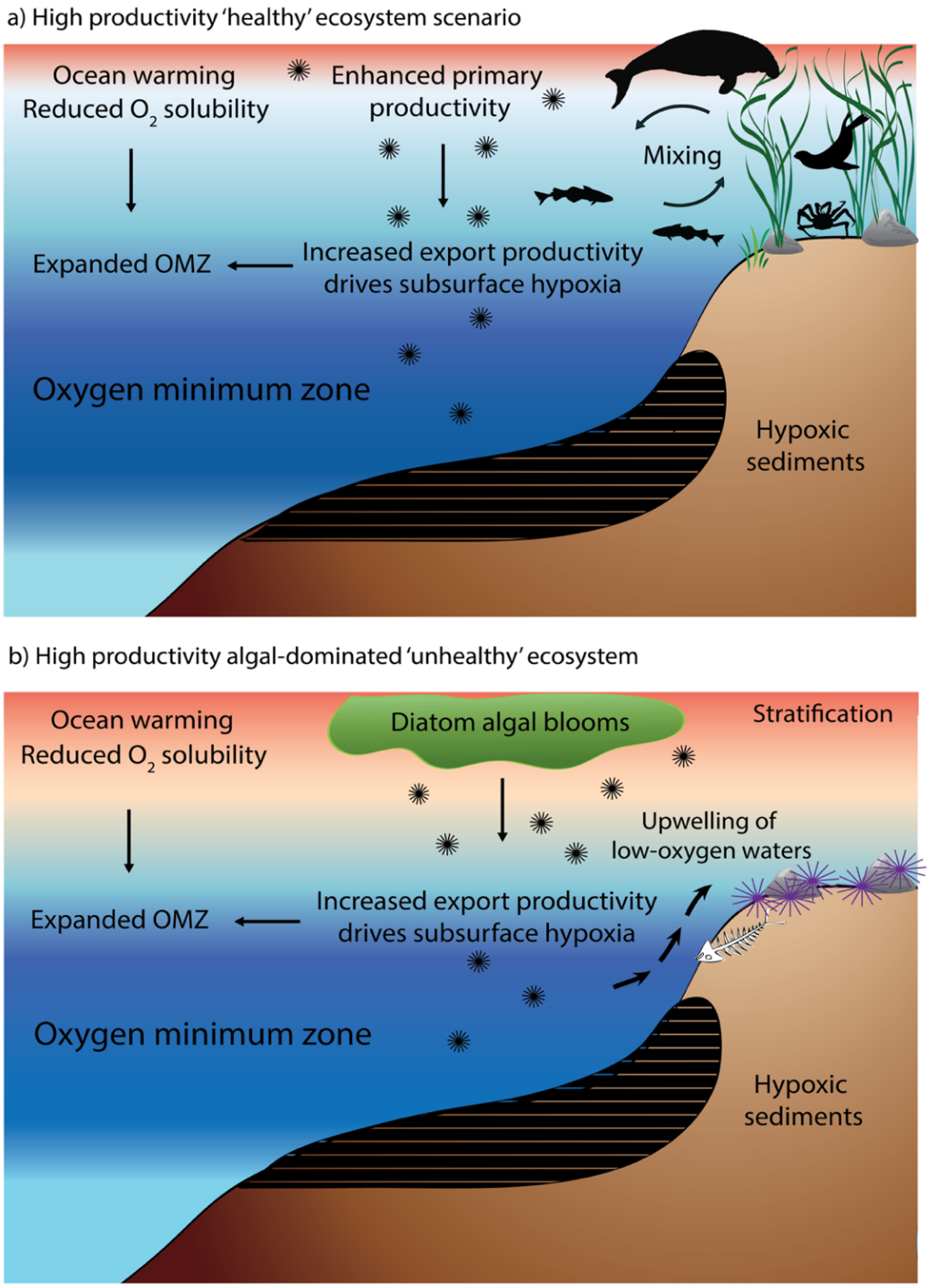

Figure S8: Contrasting scenarios for coastal ecosystems during periods of OMZ expansion, such as occurred during the Bølling-Allerød and early Holocene. Paleoceanographic reconstructions indicate ocean warming and an expansion/intensification in sedimentary hypoxia at depths between 400-1600 meters (indicated by dark blue shading), concurrent with increased burial of biosilica (diatoms) and organic carbon; however little information on the composition of coastal marine ecosystems is currently available. In the 'healthy' scenario (a), favorable conditions—such as high nutrient availability, mixing, and a stable but shallow warm surface layer—promote high primary productivity which supports a thriving ecosystem; adequate mixing keeps the upper ocean well ventilated while excess carbon export drives subsurface deoxygenation. In the 'unhealthy' scenario (b) abrupt ocean warming leads to heat stress, stratification, and a system dominated by diatom algal blooms, which deplete subsurface oxygen as sinking organic material is respired. Figure adapted and modified from (8).

Table S1. Ages for earliest archaeological sites in North America and Beringia

Site	General Location	Latitude (N)	Longitude (W)	Earliest 14C age (kyr BP)	Calibrated minimum age (ka)	Calibrated maximum age (ka)	Calibrated mean age (ka)	Primary reference for site/most recent radiocarbon age	Compilation reference
North of Ice Sheets									
Bluefish Cave	Yukon Canada	67.2	140.8	19.65 ± 0.13	23.31	24.04	23.67	Bourgeon et al., 2017	Beccera-Valdivia & Higham 2020
Swan Point	Alaska	63.3	146.0	12.50 ± 0.15	14.15	14.65	14.40	Holmes et al., 2011	Beccera-Valdivia & Higham 2020
Berelekh	Eastern Siberia	70.5	144.0	12.35 ± 0.06	13.84	14.32	14.08	Pitulko et al., 2014	Beccera-Valdivia & Higham 2020
Little John (KdVo-6)	SW Yukon	62.5	140.9	12.02 ± 0.07	13.72	13.89	14.05	Easton et al., 2009	
Walker Road	Alaska	64.0	149.2	11.82 ± 0.20	13.08	14.95	14.01	Goebel et al., 1996	Beccera-Valdivia & Higham 2020
Broken Mammoth	Alaska	64.3	146.1	11.77 ± 0.22	13.26	14.13	13.69	Holmes et al., 2001	Beccera-Valdivia & Higham 2020
Dry Creek	Alaska	63.9	149.0	11.58 ± 0.04	13.35	13.70	13.53	Graf et al., 2015	Beccera-Valdivia & Higham 2020
Moose Creek	Alaska	64.1	149.1	11.19 ± 0.06	12.98	13.74	13.36	Powers et al., 1989	Beccera-Valdivia & Higham 2020
Owl Ridge	Alaska	64.0	149.6	11.06 ± 0.06	12.75	14.32	13.53	Graf et al., 2019	Beccera-Valdivia & Higham 2020
Mead	Alaska	64.3	146.1	11.46 ± 0.05	13.01	13.52	13.27	Potter et al., 2011	Beccera-Valdivia & Higham 2020
Ushki Lake	Kamchatka	56.2	160.0	11.82 ± 0.10	12.86	13.44	13.15	Goebel et al., 2003	Beccera-Valdivia & Higham 2020
Mesa	Alaska	68.4	155.8	11.66 ± 0.08	9.36	13.91	11.63	Kunz et al., 1994	Beccera-Valdivia & Higham 2020
South of Ice Sheets									
Chiquihuite Cave	Mexico	24.6	101.1	27.93 ± 0.08	31.41	33.15	32.28	Ardelean et al, 2020	Beccera-Valdivia & Higham 2020
White Sands	New Mexico	32.8	106.3	22.86 ± 32	20.53	23.62	22.08	Bennett et al., 2021	
Gault	Texas	30.9	97.7	21.70 ± 1.4	17.39	26.44	21.92	Williams et al., 2018	Beccera-Valdivia & Higham 2020
Meadowcroft Rockshelter	Pennsylvania	40.3	80.5	16.18 ± 0.98	18.62	24.34	21.48	Adovasio et al., 1998	Beccera-Valdivia & Higham 2020
Cactus Hill	Virginia	37.0	77.3	18.30 ± 1.4	18.97	20.59	19.78	Feathers et al., 2006/8	Beccera-Valdivia & Higham 2020
Cooper's Ferry	Idaho	45.9	116.4	13.17 ± 0.07	15.28	16.56	15.92	Davis et al., 2019	Beccera-Valdivia & Higham 2020
Debra Friedkin	Texas	30.9	97.7	16.65 ± 1.075	14.69	16.33	15.51	Waters et al., 2018	Beccera-Valdivia & Higham 2020
Hebior	Wisconsin	42.6	88.0	12.59 ± 0.05	13.98	15.62	14.80	Overstreet et al., 2003	Beccera-Valdivia & Higham 2020
Page-Ladson	Florida	30.2	84.0	13.945 ± 0.05	14.45	14.71	14.58	Halligan et al., 2016	Beccera-Valdivia & Higham 2020
Lindsay	Montana	47.2	105.1	12.395 ± 0.055	13.95	14.63	14.29	Hill et al., 1998	Beccera-Valdivia & Higham 2020
Paisley Caves	Oregon	42.8	120.7	12.40 ± 0.06	13.78	14.76	14.27	Jenkins et al., 2014	Beccera-Valdivia & Higham 2020
Wally's Beach	Alberta Canada	49.4	114.1	11.53 ± 0.05	13.22	13.34	13.28	Waters et al., 2015	Beccera-Valdivia & Higham 2020
Lubbock Lake	Texas	33.6	101.9	12.65 ± 0.29	12.77	13.79	13.28	Grayson et al., 2015	Beccera-Valdivia & Higham 2020
Bonneville Estates Rockshelter	Nevada	40.3	114.1	12.39 ± 0.04	12.57	12.74	12.66	Goebel et al., 2007	Beccera-Valdivia & Higham 2020
Buhl	Idaho	42.7	114.8	10.675 ± 0.095	12.42	12.74	12.58	Green et al., 1998	Beccera-Valdivia & Higham 2020
Clovis Sites									
Sheriden Cave	Ohio	41.0	83.3	12.84 ± 0.10	13.40	14.85	14.12	Waters et al., 2009	Beccera-Valdivia & Higham 2020
Aubrey	Texas	33.4	97.8	11.59 ± 0.09	13.25	14.75	14.00	Ferring 2001	Beccera-Valdivia & Higham 2020
El Fin del Mundo	Mexico	29.7	111.8	11.55 ± 0.06	13.47	14.14	13.80	Sanchez et al., 2014	Beccera-Valdivia & Higham 2020
Blackwater Draw	New Mexico	34.3	103.3	12.79 ± 0.16	12.68	13.44	13.06	Haynes et al., 1995	Beccera-Valdivia & Higham 2020
Dent	Colorado	40.3	104.8	11.155 ± 0.05	12.42	13.55	12.98	Deviese et al., 2018	Beccera-Valdivia & Higham 2020
Murray Springs	Arizona	32.2	110.3	11.19 ± 0.18	12.62	13.02	12.82	Haynes et al., 2007	Beccera-Valdivia & Higham 2020
Anzick	Montana	46.0	110.7	10.915 ± 0.05	12.49	13.18	12.83	Beccera-Valdivia et al., 2018	Beccera-Valdivia & Higham 2020
Domebo	Oklahoma	35.0	98.3	10.96 ± 0.03	12.71	12.91	12.81	Hofman et al., 1988	Beccera-Valdivia & Higham 2020
Shawnee-Minisink	Pennsylvania	41.0	75.1	11.02 ± 0.03	12.65	12.91	12.78	McNett et al., 1977	Beccera-Valdivia & Higham 2020
Colby	Wyoming	44.0	107.9	10.95 ± 0.03	12.35	13.17	12.76	Frison et al., 1986	Beccera-Valdivia & Higham 2020
Jake Bluff	Oklahoma	36.6	99.5	10.885 ± 0.035	12.65	12.78	12.71	Bement & Carter 2003	Beccera-Valdivia & Higham 2020
Lange/Ferguson	South Dakota	43.3	102.1	11.11 ± 0.04	11.11	14.29	12.70	Hannus 2018	Beccera-Valdivia & Higham 2020
Lehner	Arizona	31.4	110.1	12.0 ± 0.45	9.39	13.58	11.48	Haynes 1992	Beccera-Valdivia & Higham 2020
Coastal Sites									
CA-SMI-261 Daisy Cave	Channel Islands	34.0	120.2	15.78 ± 0.12	18.53	18.81	18.67	Erlandson et al., 1996	McLaren et al., 2020
EkTb-9	Triquet Island	51.8	128.3		13.70	14.00	13.85	Gavreau & McLaren 2017	McLaren et al., 2020
Manis Matodon	Olympic Peninsula	48.0	123.1	11.96 ± 0.02	13.76	13.86	13.81	Waters et al., 2011	McLaren et al., 2020
EjTa-4	Calvert Island	51.7	128.1	11.44 ± 0.025	13.26	13.32	13.29	McLaren et al., 2018	McLaren et al., 2020
Devil's Kitchen	Oregon Coast	43.0	124.3	11.60 ± 0.04	12.63	13.44	13.04	Curteman 2015	McLaren et al., 2020
EaSh-81	Quadra Island	50.2	125.2		12.90	13.00	12.95	Fedje et al., 2018a	McLaren et al., 2020
CA-SRI-173 Arlington Springs	Channel Islands	34.0	120.1	11.58 ± 0.05*	12.70	13.02	12.86	Johnson et al., 2002	McLaren et al., 2020
EbSh-98	Quadra Island	50.2	125.2	10.94 ± 0.06	12.72	12.97	12.85	Fedje et al., 2018a	McLaren et al., 2020
K1 cave	Haida Gwaii	52.9	132.5	10.96 ± 0.035	12.73	12.90	12.81	Fedje et al., 2011a	McLaren et al., 2020
EbSh-1	Quadra Island	50.2	125.2	10.74 ± 0.07	12.57	12.74	12.66	Fedje et al., 2018a	McLaren et al., 2020
Gaadu Din 1	Haida Gwaii	52.3	131.5	10.615 ± 0.03	12.55	12.60	12.58	Fedje et al., 2011a	McLaren et al., 2020
Bear Creek	Puget Sound	47.6	120.1	10.49 ± 0.03	12.37	12.67	12.52	Kopperl 2016	McLaren et al., 2020
Gaadu Din 2	Haida Gwaii	52.3	131.5	10.53 ± 0.02	12.43	12.55	12.49	Fedje et al., 2011	McLaren et al., 2020
Indian Sands	Oregon Coast	42.1	124.2	10.43 ± 0.015	11.69	12.93	12.31	Davis 2008	McLaren et al., 2020
DhRn-13	Stave Watershed	49.4	122.3		12.07	12.38	12.23	McLaren et al., 2020	McLaren et al., 2020
PAIC-49 Richard's Ridge	Cedros Island, Baja CA	28.0	115.1	10.75 ± 0.03*	12.04	12.43	12.23	Des Lauriers et al., 2017	McLaren et al., 2020
DhRn-18	Stave Watershed	49.4	122.3	10.35 ± 0.03	12.04	12.39	12.21	McLaren 2017	McLaren et al., 2020
DhRo-11	Stave Watershed	49.4	122.3		12.00	12.38	12.19	McLaren et al., 2020	McLaren et al., 2020
DhRo-16	Stave Watershed	49.4	122.3	10.29 ± 0.05	11.83	12.38	12.11	McLaren 2017	McLaren et al., 2020
Shuka Kaa/On Your Knees Cave	Southeast Alaska	56.3	133.6	10.30 ± 0.05	11.83	12.46	12.08	Dixon et al., 2014	
CA-SRI-723	Channel Islands	33.6	120.1	10.94 ± 0.05*	11.93	12.17	12.05	Rick et al., 2013	McLaren et al., 2020
CA-SMI-679	Channel Islands	34.0	120.2	10.8 ± 0.05	11.71	12.20	11.96	Erlandson et al., 2011	McLaren et al., 2020
DhRn-29	Stave Watershed	49.4	122.3	10.37 ± 0.04	11.29	12.46	11.88	McLaren 2017	McLaren et al., 2020
CA-SMI-678	Channel Islands	34.0	120.2	10.95 ± 0.05	11.40	12.20	11.80	Erlandson et al., 2011	McLaren et al., 2020
CA-SRI-512	Channel Islands	34.0	120.1	10.2 ± 0.05	11.41	12.00	11.71	Erlandson, Rick, et al., 2011	McLaren et al., 2020
CA-SRI-26	Channel Islands	34.0	120.1	10.7 ± 0.04	11.41	11.98	11.70	Erlandson, Rick, & Jew 2011	McLaren et al., 2020
CA-SMI-701	Channel Islands	34.0	120.2	10.7 ± 0.04	11.41	11.73	11.57	Erlandson et al., 2013	McLaren et al., 2020
CA-SRI-997	Channel Islands	34.0	120.0	10 ± 0.03	11.27	11.74	11.51	Gill et al. 2021	
CA-SRI-706	Channel Islands	33.6	120.1	10.6 ± 0.07*	11.24	11.62	11.43	Rick et al., 2013	McLaren et al., 2020
CA-SRI-725	Channel Islands	33.6	120.1	10.59 ± 0.05*	11.22	11.36	11.29	Rick et al., 2013	McLaren et al., 2020
CA-SRI-708	Channel Islands	33.6	120.0	10.4 ± 0.05*	10.79	11.25	11.02	Rick et al., 2013	McLaren et al., 2020

* = requires marine reservoir correction

Latitude/longitude values have been rounded to protect archaeological sites from vandalism or looting.

Table S1. Summary of archaeological sites discussed and plotted in Fig. 5. For additional site and reference information, see attached Dataset S1.

#	Core	Location	Lat (°)	Lon (°)	Elev/Depth (m)	Reference	Proxy	Deglacial resolution (yr)
1	SO202-18-6	Bering Sea	60.1	179.4	1105	Meheust et al., 2018	$U^{K'}_{37}$	80
2	SO201-2-114KL	Western Bering Sea	59.3	167.0	-1376	Meyer et al., 2016	TEX_{86}	150
3	SO201-2-114KL	Western Bering Sea	59.3	167.0	-1376	Max et al., 2012	$U^{K'}_{37}$	170
4	EW0408-85JC	Gulf of Alaska	59.6	-144.2	-682	Praetorius et al., 2015	$U^{K'}_{37}$	100
5	U1419	Gulf of Alaska	59.5	-144.1	-698	Romero et al., 2022	$U^{K'}_{37}$	155
6	EW0408-87JC	Gulf of Alaska	58.8	-144.5	-3680	Praetorius et al., 2020	$U^{K'}_{37}$	200
7	SO201-2-101KL	Bering Sea	58.8	170.7	-630	Riethdorf et al., 2013	Mg/Ca	160
8	EW0408-66JC	Gulf of Alaska	58.5	-137.2	-426	Praetorius et al., 2016	$U^{K'}_{37}$	50
9	EW0408-26JC	Gulf of Alaska	57.6	-136.7	-1623	Praetorius et al., 2016	$U^{K'}_{37}$	50
10	SO201-2-85KL	Bering Sea	57.5	170.4	-968	Riethdorf et al., 2013	Mg/Ca	225
11	SO201-2-85KL	Bering Sea	57.5	170.4	-968	Max et al., 2012	$U^{K'}_{37}$	170
12	SO201-2-77KL	Bering Sea	56.3	170.7	-2135	Max et al., 2012	$U^{K'}_{37}$	190
13	SO201-2-77KL	Bering Sea	56.3	170.7	-2135	Riethdorf et al., 2013	Mg/Ca	310
14	SO202-27-6	Gulf of Alaska	54.2	-149.6	-2919	Meheust et al., 2018	$U^{K'}_{37}$	880*
15	SO201-2-12KL	Northwestern Pacific	54.0	162.4	-2145	Meyer et al., 2016	TEX_{86}	140
16	SO201-2-12KL	Northwestern Pacific	54.0	162.4	-2145	Riethdorf et al., 2013	Mg/Ca	80
17	SO201-2-12KL	Northwestern Pacific	54.0	162.4	-2145	Max et al., 2012	$U^{K'}_{37}$	70
18	U1340	Bering Sea	53.4	179.5	-1294	Schlung et al., 2013	$U^{K'}_{37}$	410*
19	XP07-C9	Okhotsk Sea	52.3	146.0	-1431	Harada et al., 2012	$U^{K'}_{37}$	340
20	MR06-04-PC7	Okhotsk Sea	51.3	149.2	-1247	Seki et al., 2009	TEX_{86}	1500*
21	SO202-07-6	Northwestern Pacific	51.3	167.7	-2340	Meheust et al., 2018	$U^{K'}_{37}$	870*
22	XP98-PC-2	Okhotsk Sea	50.4	148.3	-1258	Seki et al., 2004	$U^{K'}_{37}$	670*
23	XP98-PC-4	Okhotsk Sea	49.5	146.1	-664	Seki et al., 2004	$U^{K'}_{37}$	640*
24	MR00K03-PC-04	Okhotsk Sea	49.4	153.0	-1821	Harada et al., 2004	$U^{K'}_{37}$	310
25	LV29-114-3	Okhotsk Sea	49.4	152.9	-1765	Max et al., 2012	$U^{K'}_{37}$	230
26	LV29-114-3	Okhotsk Sea	49.4	152.9	-1765	Riethdorf et al., 2013	Mg/Ca	110
27	MD02-2496	Vancouver margin	49.0	-127.0	-1243	Taylor et al., 2014	Mg/Ca	110
28	MD02-2496	Vancouver margin	49.0	-127.0	-1243	Taylor et al., 2014	Mg/Ca	80
29	JT96-09PC	Vancouver margin	48.9	-126.9	-920	Kienast & McKay 2001	$U^{K'}_{37}$	90
30	MR00K03-PC-01	Northwestern Pacific	46.3	152.5	-2793	Harada et al., 2004	$U^{K'}_{37}$	200
31	MR9702-St-8s	Okhotsk Sea	44.8	170.2	-1780	Harada et al., 2004	$U^{K'}_{37}$	750*
32	MD01-2412	Okhotsk Sea	44.5	145.0	-1225	Harada et al., 2006	$U^{K'}_{37}$	210
33	MR06-04-PC04	Okhotsk Sea	44.5	145.0	-1225	Harada et al., 2012	$U^{K'}_{37}$	110
34	W8709A-8TC	Northeastern Pacific	42.2	-127.7	-3111	Prahl et al., 1995	$U^{K'}_{37}$	1010*
35	GH02-1030	Northwestern Pacific	42.2	144.2	-1212	Inagaki et al., 2009	$U^{K'}_{37}$	390
36	ODP 1019	California margin	41.7	-124.9	-980	Barron et al., 2003, Herbert et al., 2003	$U^{K'}_{37}$	70
37	ODP 1020	California margin	41.0	-126.4	-3042	Herbert et al., 2001	$U^{K'}_{37}$	640*
38	PC-6	Japan margin	40.4	143.5	-2215	Minoshima et al., 2007	$U^{K'}_{37}$	250
39	MR98-05-St5	Central Pacific	40.0	165.0	-5498	Harada et al., 2004	$U^{K'}_{37}$	1300*
40	MR98-05-St6	Central Pacific	37.5	162.7	-3130	Harada et al., 2004	$U^{K'}_{37}$	2800*
41	MD01-2421	Northwestern Pacific	36.0	141.8	-2224	Yamamoto et al., 2005	$U^{K'}_{37}$	150
42	ODP 1017	California margin	34.5	-121.1	-955	Pak et al., 2012	Mg/Ca	160
43	ODP 1017	California margin	34.5	-121.1	-955	Seki et al., 2002	$U^{K'}_{37}$	250
44	ODP 1016	California margin	34.5	-122.3	-3834	Yamamoto et al., 2007	$U^{K'}_{37}$	1120*
45	ODP 893	Santa Barbara Basin	34.3	-120.0	-575	Hendy 2010	foram assemblages	60
46	ODP 1014	California margin	32.8	-118.9	-1165	Yamamoto et al., 2007	$U^{K'}_{37}$	1470*
47	KT92-17 St. 14	Japan margin	32.6	138.6	-3252	Sawada and Handa, 1998	$U^{K'}_{37}$	440*
48	ODP 1012	California margin	32.3	-118.4	-1783	Herbert et al., 2001	$U^{K'}_{37}$	610*
49	KY07-04-01	Japan margin	31.6	128.9	-758	Kubota et al., 2010	Mg/Ca	100
50	MD98-2195	East China Sea	31.6	129.0	-746	Ijiri et al., 2005	$U^{K'}_{37}$	160
51	MD02-2515	Guaymas Basin	27.5	-112.1	-881	McClymont et al., 2012	$U^{K'}_{37}$	80
52	MD02-2515	Guaymas Basin	27.5	-112.1	-881	McClymont et al., 2012	TEX_{86}	85
53	LaPaz 21P	Baja Penisula	23.0	-109.5	-624	Herbert et al., 2001	$U^{K'}_{37}$	1320*
54	17940	South China Sea	20.1	117.4	-1968	Pelejero et al., 1999	$U^{K'}_{37}$	150
55	ODP 1144	South China Sea	20.1	117.6	-2037	Wei et al, 2007	Mg/Ca	300
56	GIK17927-2	South China Sea	17.3	119.5	-2804	Sadatzki et al., 2016	$U^{K'}_{37}$	150
57	GIK17954-2	South China Sea	14.8	111.5	-1520	Pelejero et al., 1999	$U^{K'}_{37}$	1070*
58	MD97-2141	Sulu Sea	8.8	121.3	-3633	Rosenthal et al., 2003	Mg/Ca	70
59	MD02-2529	Eastern equatorial Pacific	8.2	-84.1	-1619	Leduc et al., 2007	$U^{K'}_{37}$	260
60	ME0005A-43JC	Eastern equatorial Pacific	7.9	-83.6	-1368	Benway et al., 2006	Mg/Ca	220
61	MD01-2390	South China Sea	6.6	113.4	-1545	Steinke et al., 2008	$U^{K'}_{37}$	200
62	MD01-2390	South China Sea	6.6	113.4	-1545	Steinke et al., 2008	Mg/Ca	200
63	MD98-2181	West Pacific warm pool	6.3	125.8	-2114	Stott et al., 2007	Mg/Ca	60
64	TR163-22	Eastern equatorial Pacific	0.5	-92.4	-2830	Lea et al., 2006	Mg/Ca	250
65	ME0005A-24JC	Eastern equatorial Pacific	0.0	-86.5	-2941	Kienast et al., 2006	$U^{K'}_{37}$	150

* denotes datasets with deglacial resolution that exceeds the 400-yr cutoff; used these datasets for LGM-Holocene estimates only

Table S2. Summary of marine sediment cores used in the North Pacific SST compilation (Fig. 4). For additional information on SST data and age models, see Dataset S4.

Legends for Data Files:

Dataset S1 (Microsoft Excel format): Metadata, references, and radiocarbon data for archaeological sites listed in Table S1.

Dataset S2 (Microsoft Excel format): Age models recalibrated using the Marine20 calibration for the following cores: EW0408-66JC, EW0408-87JC, EW0408-26JC, JT96-09JPC, ODP1019, with variable marine reservoir corrections that generally follow those applied in (37).

Dataset S3 (Microsoft Excel format): New alkenone-derived $\%C_{37:4}$ records from the following marine sediment cores in the Gulf of Alaska: EW0408-85JC, EW0408-66JC, EW0408-87JC, EW0408-26JC.

Dataset S4 (Microsoft Excel format): Metadata, references, and age model information for North Pacific marine sediment cores used in the SST compilation (Fig. 4, Table S2).

Dataset S5 (Microsoft Excel format): Average Northeast Pacific SST stacks.

References:

1. S.-O. Rasmussen *et al.*, A stratigraphic framework for abrupt climatic changes during the Last Glacial period based on three synchronized Greenland ice-core records: Refining and extending the INTIMATE event stratigraphy. *QSR* **106**, 14-28 (2014).
2. J.-M. Erlandson *et al.*, The kelp highway hypothesis: marine ecology, the coastal migration theory, and the peopling of the Americas. *The Journal of Island and Coastal Archaeology* **2**, 161-174 (2007).
3. J.-M. Erlandson, T.-J. Braje, K.-M. Gill, M.-H. Graham, Ecology of the kelp highway: Did marine resources facilitate human dispersal from Northeast Asia to the Americas? *Journal of Island & Coastal Archaeology* **10,** 392-411 (2015).
4. J. Dobson, G. Spada, G. Galassi, The Bering Transitory Archipelago: Stepping stones for the first Americans. *Comptes Rendus Geoscience – Sciences de la Planete* **353**, 55-65 (2021).
5. C.-D. Bullen, A.-A. Campos, E.-J. Gregr, I. McKechnie, K.-M.-A. Chan, The ghost of a giant—Six hypotheses for how an extinct megaherbivore structured kelp forests across the North Pacific rim. *Global Ecol. Biogeogr.* **30**, 2101- 2118 (2021).
6. D.-P. Domning, J. Thomason, D.-G. Corbett, Steller's sea cow in the Aleutian Islands. *Marine Mammal Science*, **23(4)**, 976-983 (2007).
7. K. Filbee-Dexter, T. Wernberg, S. Fredriksen, K.-M. Norderhaug, M.-F. Pedersen, Arctic kelp forests: Diversity, resilience, and future. *Global and Planetary Change* **172,** 1-14 (2019).
8. S.-K. Praetorius *et al.*, North Pacific deglacial hypoxic events linked to abrupt ocean warming. *Nature* **527**, 362-366 (2015).
9. S.-E. Moffitt, T.-M. Hill, P.-D. Roopnarine, J.-P. Kennett. Response of seafloor ecosystems to abrupt global climate change. *PNAS* **112, 45**, 4684-4689 (2015a).
10. A.-M. Springer, P. McRoy, M. Flint, The Bering Sea green belt: shelf edge processes and ecosystem production. *Fish. Oceanogr.* **5:3/4**, 205-223 (1996).

11. C. Lopes, M. Kucera, A.-C. Mix, Climate change decouples oceanic primary and export productivity and organic carbon burial, *PNAS* **112(2)**, 332-335 (2015).
12. K.-A. Grimm, C.-B. Lange, A.-S. Gill. Self-sedimentation of phytoplankton blooms in the geological record. *Sedimentary Geology* **110**, 151-161 (1997).
13. B.-A. Potter *et al.* Early colonization of Beringia and Northern North America: Chronology, routes, and adaptive strategies. *Quat. Int*. **444**, 36-55 (2017).
14. B.-A. Potter *et al.* Current evidence allows multiple models for the peopling of the Americas. *Sci Adv* **4**, eaat5473 (2018).
15. J. Erlandson *et al.*, An archaeological and paleontological chronology for Daisy Cave (CA-SMI-261), San Miguel Island, California. *Radiocarbon* **38 #2**, 355-373 (1996).
16. D. McLaren *et al.* Late Pleistocene archaeological discovery models on the Pacific Coast of North America. *PaleoAmerica*, **6:1**, 43-63 (2020).
17. Braje, T. Costello, J.G., Erlandson, J.M., Johnson, J.R., Morris, D.P., Perry, J.E,. Rick, T.C. Technical report. Channel Islands National Park Archaeological Overview and Assessment. Glassow, M.A. (editor) (2014).
18. M.-H. Davies *et al.*, The deglacial transition on the southeastern Alaska Margin: Meltwater input, sea level rise, marine productivity, and sedimentary anoxia. *Paleoceanography* **26**, (2011).
19. H. Kuehn, *et al.*, Laminated sediments in the Bering Sea reveal atmospheric teleconnections to Greenland climate on millennial to decadal timescales during the last deglaciation, *Clim. Past* **10**, 2215–2236, (2014).
20. O.-C. Romero *et al.*, Orbital and suborbital variations of productivity and sea surface conditions in the Gulf of Alaska during the past 54,000 years: Impact of iron fertilization by icebergs and meltwater. *Paleoceanography & Paleoclimatology* **37** e2021PA004385 (2022).
21. S.-K. Praetorius *et al.*, The role of Northeast Pacific meltwater events in deglacial climate change. *Science Advances* **6**: eaay2915 (2020).
22. S.-K. Praetorius, *et al.*, Interaction between climate, volcanism, and isostatic rebound in Southeast Alaska during the last deglaciation. *Earth Planet. Sci. Lett.* **452**, 79–89 (2016).
23. M.-A. Taylor, I.-L. Hendy, D.-K. Pak., Deglacial ocean warming and marine margin retreat of the Cordilleran Ice Sheet in the North Pacific Ocean. *Earth and Planetary Science Letters* **403**, 89–98, (2014).
24. S.-S. Kienast, J.-L. McKay, Sea surface temperatures in the subarctic northeast Pacific reflect millennial-scale climate oscillations during the last 16 kyrs. *Geophys. Res. Lett.* **28**, 1563–1566 (2001).
25. J.-A. Barron, L. Heusser, T. Herbert, M. Lyle. High-resolution climatic evolution of coastal northern California during the past 16,000 years. *Paleoceanography* **18(1)**, (2003).
26. T.-D. Herbert, Alkenone paleotemperature determinations in *Treatise on Geochemistry*, H. Elderfield, H.D. Holland, K.K Turekian, Eds. Elsevier, pp. 391-432 (2003).
27. J.-M. Adovasio, D.-R. Pedler, J. Donahue, R. Stuckenrath, Two decades of debate on Meadowcroft Rockshelter. *North American Archaeologist* **19**, 317–341 (1998).

28. C.-F. Ardelean *et al.*, Evidence of human occupation in Mexico around the Last Glacial Maximum. *Nature* **584**, 87-92 (2020).
29. L. Becerra-Valdivia *et al.* Reassessing the chronology of the archaeological site of Anzick. *Proc. Natl. Acad. Sci.* **115**, 7000–7003 (2018).
30. L. Becerra-Valdivia & T. Higham. The timing and effects of the earliest human arrivals in North America. *Nature* DOI:10.1038/s41586-020-2491-6 (2020).
31. L.-C. Bement, B.-J. Carter, Clovis bison hunting at the Jake Bluff site, NW Oklahoma. *Current Research in the Pleistocene* **20**, 5–7 (2003).
32. M.-R. Bennett *et al.*, Evidence of humans in North America during the Last Glacial Maximum. *Science* **373**, 1528-1531 (2021).
33. L. Bourgeon, A. Burke, T. Higham. Earliest human presence in North America dated to the Last Glacial Maximum: New radiocarbon dates from Bluefish Caves, Canada. *PLoS ONE* **12 (1)**, e0169486 (2017).
34. J. Curteman, Geoarchaeological investigations at the Devils Kitchen Site (35CS9), Southern Oregon Coast. MA thesis, Department of Anthropology, Oregon State University, Corvallis OR (2015).
35. L. Davis, New support for a Late Pleistocene-aged coastal occupation at the Indian Sands Site, Oregon. *Current Research in the Pleistocene* **25**, 74–76 (2008).
36. L. Davis *et al.*, Late Upper Paleolithic occupation at Cooper's Ferry, Idaho, USA, ~16,000 years ago. *Science* **365**, 891-897 (2019).
37. M.-L. Des Lauriers, L. Davis, J. Turnbull, J. Southon, and R. Taylor. The earliest shell fishhooks from the Americas reveal fishing technology of Pleistocene maritime foragers. *American Antiquity* **82**, 498–516 (2017).
38. T. Devièse, *et al.* Increasing accuracy for the radiocarbon dating of sites occupied by the first Americans. *Quaternary Science Research* **198**, 171–180 (2018).
39. E.-J. Dixon, *et al.* Evidence of maritime adaptation and coastal mfrom Southeast Alaska. pp. 537-548 in Owsley, D. W., and Jantz, R. L. (eds.) Kennewick Man: The Scientific Investigation of an Ancient American Skeleton, Texas A&M University Press, 669 p. (2014).
40. N.-A. Easton, D.-R. Yesner, V. Hutchinson, P. Schnurr, and C. Baker. Wisconsin Interstadial, Terminal-Pleistocene, and Early Holocene radiocarbon dates from the Little John Site, Southwest Yukon Territory, Canada. *Current Research in the Pleistocene* **26**, 47–50 (2009).
41. J.-M. Erlandson *et al.*, An archaeological and paleontological chronology for Daisy Cave (CA-SMI-261), San Miguel Island, California. *Radiocarbon* **38 #2**, 355-373 (1996).
42. J.-M. Erlandson, T. Braje. From Asia to the Americas by boat? Paleogeography, paleoecology, and stemmed points of the Northwest Pacific. *Quaternary International* **239**, 28–37 (2011).
43. J.-M. Erlandson, T. Rick, and N. Jew. CA-SRI-26: A Terminal Pleistocene Site on Santa Rosa Island, California. *Current Research in the Pleistocene* **28**, 35–37 (2011).
44. J.-M. Erlandson, *et al.* Paleoindian seafaring, maritime technologies, and coastal foraging on California's Channel Islands. *Science* **441**, 1181–1185 (2011).
45. J.-M. Erlandson, Channel Island Amol Points: A Stemmed Paleocoastal Type from Santarosae Island, Alta California. *California Archaeology* **5**, 105–121 (2013).

46. J.-K. Feathers, E.-J. Rhodes, S. Huot, J.-M. Mcavoy, Luminescence dating of sand deposits related to late Pleistocene human occupation at the Cactus Hill Site, Virginia, USA. *Quat. Geochronol.* **1**, 167–187 (2006/8).
47. D. Fedje, Q. Mackie, T. Lacourse, and D. McLaren. Younger Dryas Environments and Archaeology on the Northwest Coast of North America. *Quaternary International* **242**, 452–462 (2011a).
48. D. Fedje, Q. Mackie, N. Smith, and D. McLaren. Function, Visibility, and Interpretation of Archaeological Assemblages at the Pleistocene/Holocene Transition in Haida Gwaii. In From the Yenisei to the Yukon: Interpreting Lithic Assemblage Variability in Late Pleistocene/Early Holocene Beringia, edited by T. Goebel and I. Buvit, 408. College Station: Texas A&M University Press, 2011b.
49. D. Fedje, D. McLaren, T. James, Q. Mackie, N. Smith, J. Southon, and A. Mackie. A revised sea level history for the northern Strait of Georgia, British Columbia, Canada. *Quaternary Science Reviews* **192**, 300– 316 (2018a).
50. C.-R. Ferring, The archaeology and paleoecology of the Aubrey Clovis site (41DN479) Denton County, Texas. http://www.dtic.mil/docs/citations/ADA391588 (2001).
51. Frison, G. C. & Todd, L. C. The Colby mammoth site: Taphonomy and archaeology of a Clovis kill in northern Wyoming. (University of New Mexico Press, 1986)
52. Gavreau, A., and D. McLaren. “Long-term culture landscape development at (EkTb-9) Triquet Island, British Columbia, Canada.” Paper presented at the 50th Annual Meeting of the Canadian Archaeological Association, Ottawa, Ontario, May 10–13 (2017).
53. Gill, K., T. Braje, K. Smith, & J. Erlandson. Earliest evidence for geophyte use in North America: 11,500-year-old archaeobotanical remains from California’s Santarosae Island. American Antiquity 86(3):625-637 (2021).
54. T. Goebel, M.-R. Waters, M. Dikova, The archaeology of Ushki Lake, Kamchatka, and the Pleistocene peopling of the Americas. *Science* **301**, (2003).
55. Goebel, T., Powers, R., Bigelow, N. H. & Higgs, A. S. Walker Road. in American Beginnings: The Prehistory and Palaeoecology of Beringia (ed. West, F. H.) 356–363 (University of Chicago Press, 1996)
56. Goebel, T., Graf, K. & Rhode, D. The Paleoindian occupations at Bonneville Estates Rockshelter, Danger Cave, and Smith Creek Cave (eastern Great Basin, USA): Interpreting their radiocarbon chronologies. British Archaeological Reports (BAR) International Series 1655, 147 (2007)
57. K.-E. Graf *et al.* Dry Creek revisited: New excavations, radiocarbon dates, and sformation inform on the peopling of Eastern Beringia. *Am. Antiq.* 80, 671–694 (2015).
58. K.-E. Graf *et al.* Recent excavations at Owl Ridge, interior Alaska: Site stratigraphy, chronology, and site formation and implications for late Pleistocene archaeology and peopling of eastern Beringia. Geoarchaeology 35, 3–26 (2019).
59. Grayson, D. K. & Meltzer, D. J. Revisiting Paleoindian exploitation of extinct North American mammals. J. Archaeol. Sci. 56, 177–193 (2015)
60. Green, T. J. et al. The Buhl Burial: A Paleoindian woman from Southern Idaho. Am. Antiq. 63, 437– 456 (1998)

61. Halligan, J. J. et al. Pre-Clovis occupation 14,550 years ago at the Page-Ladson site, Florida, and the peopling of the Americas. Sci Adv 2, e1600375 (2016)
62. Hannus, L. A. Clovis Mammoth Butchery: The Lange/Ferguson Site and associated bone tool technology. (Texas A&M University Press, 2018)
63. Haynes, C. V. Geochronology of paleoenvironmental change, Clovis type site, Blackwater Draw, New Mexico. Geoarchaeology 10, 317–388 (1995)
64. Haynes, C. V. Contributions of radiocarbon dating to the geochronology of the peopling of the New World. in Radiocarbon After Four Decades 355–374 (Springer New York, 1992) New World. in Radiocarbon After Four Decades 355–374 (Springer New York, 1992)
65. Haynes, C. V. & Huckell, B. B. Murray Springs: A Clovis site with multiple activity areas in the San Pedro Valley, Arizona. (University of Arizona Press, 2007)
66. Hill, C. L. & Davis, L. B. Stratigraphy, AMS radiocarbon age, and stable isotope biogeochemistry of the Lindsay Mammoth, eastern Montana. Current Research in the Pleistocene 15, 109–112 (1998).
67. Hofman, J. L. Dating the lower member of the Domebo Formation in western Oklahoma. Current Research in the Pleistocene 5, 86–88 (1988)
68. C.-E. Holmes, Tanana River Valley archaeology circa 14,000 to 9000 B.P. *Arctic Anthropol.* 38, 154–170 (2001).
69. C.-E. Holmes, The Beringian and transitional periods in Alaska: technology of the east Beringian tradition as viewed from Swan point. in From the Yenisei to the Yukon: Interpreting Lithic Assemblage Variability in Late Pleistocene/Early Holocene Beringia (eds. Goebel, T. & Buvit, I.) 179–198 (Texas A&M University Press, 2011)
70. D.-L. Jenkins *et al.* Geochronology, archaeological context, and DNA at the Paisley Caves. In Paleoamerican Odyssey (eds. Graf, K. E., Ketron, C. V. & Waters, M. R.) 485–510 (Center for the Study of the First Americans, Texas A&M University College Station, 2014).
71. Johnson, J., T. Stafford Jr, H. Ajie, & D. Morris. 2002. Arlington SpringsrRevisited. In Proceedings of the Fifth California Islands Symposium, edited by D. Browne, K. Mitchell, and H. Chaney, 541–545. Santa Barbara, CA: Santa Barbara Museum of Natural History.
72. R. Kopperl, Results of Data Recovery at the Bear Creek Site (45K1839) King County, Washington. 27287. Seattle: SWCA Environmental Consultants (2016).
73. C.-W. McNett, B.-A. McMillan, S.-B. Marshall, The Shawnee-Minisink Site. Ann. N. Y. Acad. Sci. **288**, 282–296 (1977).
74. M.-L. Kunz, R.-E. Reanier, Paleoindians in Beringia: Evidence from Arctic Alaska. *Science* **263**, 660–662 (1994)
75. D. McLaren *et al.* Terminal Pleistocene epoch human footprints from the Pacific coast of Canada. PLoS One 13, e0193522 (2018).
76. D. McLaren, The occupational history of the Stave Watershed. In Archaeology of the Lower Fraser River Region, edited by M. Rousseau, 149–158. Burnaby: Archaeology Press, Simon Fraser University (2017).

77. D. McLaren *et al.* Late Pleistocene archaeological discovery models on the Pacific Coast of North America. *PaleoAmerica*, **6:1**, 43-63 (2020).
78. D.-F. Overstreet, M.-F. Kolb, Geoarchaeological contexts for Late Pleistocene archaeological sites with human-modified woolly mammoth remains in southeastern Wisconsin, U.S.A. *Geoarchaeology* **18**, 91–114 (2003).
79. B.-A. Potter, P.-J. Gilbert, C.-E. Holmes, B.-A. Crass, The Mead Site, a late Pleistocene - Holocene stratified site in Central Alaska. *Current Research in the Pleistocene* 28, 73–75 (2011).
80. V.-V. Pitulko, A.-E. Basilyan, E.-Y. Pavlova, The Berelekh Mammoth 'graveyard': New chronological and stratigraphical data from the 2009 field season. Geoarchaeology 29, 277–299 (2014).
81. W.-R. Powers, J.-F. Hoffecker, Late Pleistocene settlement in the Nenana Valley, Central Alaska. *Am. Antiq.* 54, 263–287 (1989).
82. T. Rick, J. Erlandson, N. Jew, & L. Reeder-Myers. Archaeological survey, paleogeography, and the search for Late Pleistocene Paleocoastal peoples of Santa Rosa Island, California. *Journal of Field Archaeology* **38**, 324– 331 (2013).
83. Sanchez, G. et al. Human (Clovis)-gomphothere (*Cuvieronius* sp.) association ~ 13,390 calibrated yBP in Sonora, Mexico. *Proc. Natl. Acad. Sci.* **111**, 10972–10977 (2014).
84. M.-R. Waters, T.-W. Stafford, B.-G. Redmond, K.-B. Tankersley, The age of the Paleoindian assemblage at Sheriden Cave, Ohio. *Am. Antiq.* **74**, 107–111 (2009).
85. Waters, M. R. et al. Pre-Clovis mastodon hunting 13,800 years ago at the Manis Site, Washington. Science 334, 351–353 (2011).
86. M.-R. Waters *et al.* Pre-Clovis projectile points at the Debra L. Friedkin site, Texas—Implications for the Late Pleistocene peopling of the Americas. Science Advances 4, eaat4505 (2018).
87. Waters, M. R., Stafford, T. W., Jr, Kooyman, B. & Hills, L. V. Late Pleistocene horse and camel hunting at the southern margin of the ice-free corridor: reassessing the age of Wally's Beach, Canada. Proc. Natl. Acad. Sci. U. S. A. 112, 4263–4267 (2015)
88. T.-J. Williams *et al.* Evidence of an early projectile point technology in North America at the Gault Site, Texas, USA. *Sci Adv* **4**, eaar5954 (2018).
89. J.-A. Barron, L. Heusser, T. Herbert, M. Lyle. High-resolution climatic evolution of coastal northern California during the past 16,000 years. *Paleoceanography* **18(1)**, (2003).
90. H. M. Benway, J. F. McManus, D. W. Oppo, J. L. Cullen, Hydrographic changes in the eastern subpolar North Atlantic during the last deglaciation. *Quat. Sci. Rev.* **29**, 3336–3345 (2010).
91. N. Harada, N. Ahagon, M. Uchida, M. Murayama, Northward and southward migrations of frontal zones during the past 40 kyr in the Kuroshio-Oyashio transition area. *Geochem. Geophys. Geosyst.* **5**, Q09004 (2004).
92. N. Harada, N. Ahagon, T. Sakamoto, M. Uchida, M. Ikehara, Y. Shibata, Rapid fluctuation of alkenone temperature in the southwestern Okhotsk Sea during the past 120 ky. *Global Planet. Change* **53**, 29–46 (2006).
93. N. Harada, *et al.* Sea surface temperature changes in the Okhotsk Sea and adjacent North Pacific during the last glacial maximum and deglaciation. *Deep-Sea Research II* **61-64**, 93-105 (2012).

94. I.-L. Hendy, The paleoclimatic response of the Southern Californian Margin to the rapid climate change of the last 60ka: A regional overview. *Quat. Int.* **215**, 62–73 (2010).
95. T.-D. Herbert, *et al.* Collapse of the California Current during glacial maximum linked to climate change on land. *Science* **293**, 71-76 (2001).
96. T.-D. Herbert, Alkenone paleotemperature determinations in *Treatise on Geochemistry*, H. Elderfield, H.D. Holland, K.K Turekian, Eds. Elsevier, pp. 391-432 (2003).
97. S.-S. Kienast, J.-L. McKay, Sea surface temperatures in the subarctic northeast Pacific reflect millennial-scale climate oscillations during the last 16 kyrs. *Geophys. Res. Lett.* **28**, 1563–1566 (2001).
98. M. Kienast, *et al.* Eastern Pacific cooling and Atlantic overturning circulation during the last deglaciation. *Nature* **443**, 846–849 (2006).
99. Y. Kubota, K. Kimoto, R. Tada, H. Oda, Y. Yokoyama, H. Matsuzaki, variations of East Asian summer monsoon since the last deglaciation based on Mg/Ca and oxygen isotope of planktic foraminifera in the northern East China Sea. *Paleoceanography* **25**, PA4205 (2010).
100. M. Inagaki, M. Yamamoto, Y. Igarashi, K. Ikehara, Biomarker records from Core GH02-1030 off Tokachi in the Northwestern Pacific over the Last 23,000 years: Environmental Changes during the Last Deglaciation. *J. of Oceanography* **65**, 847-858 (2009).
101. A. Ijiri, L. Wang, T. Oba, H. Kawahata, C. Y. Huang, C. Y. Huang, Paleoenvironmental changes in the northern area of the East China Sea during the past 42,000 years. *Palaeogeogr. Palaeoclimatol. Palaeoecol.* **219**, 239–261 (2005).
102. G. Leduc, L. Vidal, K. Tachikawa, F. Rostek, C. Sonzogni, L. Beaufort, E. Bard, Moisture transport across Central America as a positive feedback on abrupt climatic changes. *Nature* **445**, 908–911 (2007).
103. D.-W. Lea, D.-K. Pak, C.-L. Belanger, H.-J. Spero, M.-A. Hall, N.-J. Shackleton, Paleoclimate history of Galápagos surface waters over the last 135,000yr. *Quat. Sci. Rev.* **25**, 1152–1167 (2006).
104. L. Max, *et al.* Sea surface temperature variability and sea-ice extent in the subarctic northwest Pacific during the past 15,000 years. *Paleoceanography* **27**, PA3213 (2012).
105. E.-L. McClymont, R. S. Ganeshram, L. E. Pichevin, H. M. Talbot, B. E. van Dongen, R. C. Thunell, A. M. Haywood, J. S. Singarayer, P. J. Valdes, Sea-surface temperature records of Termination 1 in the Gulf of California: Challenges for seasonal and interannual analogues of tropical pacific climate change. *Paleoceanography* **27**, PA2202 (2012).
106. M. Méhéust, R. Stein, K. Fahl, R. Gersonde, Sea-ice variability in the subarctic North Pacific and adjacent Bering Sea during the past 25 ka: new insights from IP_{25} and Uk'37 proxy records. *Arktos* **4:8** (2018).
107. V.-D. Meyer, L. Max, J. Hefter, R. Tiedemann, G. Mollenhauer, Glacial-to-Holocene evolution of sea surface temperature and surface circulation in the subarctic northwest Pacific and the Western Bering Sea. *Paleoceanography* **31**, 916–927 (2016).
108. K. Minoshima, H. Kawahata, K. Ikehara, Changes in biological production in the mixed water region (MWR) of the northwestern North Pacific during the last 27 kyr. *Palaeogeogr. Palaeoclimatol. Palaeoecol.* **254**, 430–447 (2007).

109. D.-K. Pak, D.-W. Lea, J.-P. Kennett, Millennial scale changes in sea surface temperature and ocean circulation in the northeast Pacific, 10–60 kyr BP. *Paleoceanography* **27**, PA1212 (2012).
110. C. Pelejero, J.-O. Grimalt, S. Heilig, M. Kienast, L. Wang, High-resolution U_{37} temperature reconstructions in the South China Sea over the past 220 kyr. *Paleoceanography* **14**, 224–231 (1999).
111. S.-K. Praetorius *et al.*, North Pacific deglacial hypoxic events linked to abrupt ocean warming. *Nature* **527**, 362-366 (2015).
112. S. Praetorius, A. Mix, B. Jensen, D. Froese, G. Milne, M. Wolhowe, J. Addison, F. Prahl, Interaction between climate, volcanism, and isostatic rebound in Southeast Alaska during the last deglaciation. *Earth Planet. Sci. Lett.* **452**, 79–89 (2016).
113. S.-K. Praetorius *et al.*, The role of Northeast Pacific meltwater events in deglacial climate change. *Science Advances* **6**: eaay2915 (2020).
114. F.-G. Prahl, N. Pisias, M.-A. Sparrow, A. Sabin. Assessment of sea-surface temperature at 42°N in the California Current over the last 30,000 years. *Paleoceanography* **10(4)**, 763-773 (1995).
115. J. Riethdorf, *et al.* Deglacial development of (sub) sea surface temperature and salinity in the subarctic northwest Pacific: Implications for upper ocean stratification. *Paleoceanography*, **28**, 91-104 (2013).
116. K. Sawada, N. Handa, Variability of the path of the Kuroshio ocean current over the past 25,000 years. *Nature* **392**, 592–595 (1998).
117. S.-A. Schlung, Christina Ravelo, A., Aiello, I.W., Andreasen, D.H., Cook, M.S., Drake, M., Dyez, K.A., Guilderson, T.P., LaRiviere, J.P., Stroynowski, Z., 2013. Millennial-scale climate change and intermediate water circulation in the Bering Sea from 90 ka: a high-resolution record from IODP Site U1340. *Paleoceanography* 28(1), 54e67 (2013).
118. H. Sadatzki, M. Sarnthein, N. Andersen, Changes in monsoon-driven upwelling in the South China Sea over glacial Terminations I and II: a multi-proxy record. *Int. J. Earth Sci.* **105**, 1273-1285 (2016).
119. O. Seki, *et al.* Large changes in seasonal sea ice distribution and productivity in the Sea of Okhotsk during the deglaciations. *G^3* **10**, Q10007, (2009).
120. O. Seki, K. Kawamura, M. Ikehara, T. Nakatsuka, T. Oba, Variation of alkenone sea surface temperature in the Sea of Okhotsk over the last 85 kyrs. *Org. Geochem.* **35** (3), 347e354 (2004).
121. O. Seki, R. Ishiwatari, K. Matsumoto, Millennial climate oscillations in NE Pacific surface waters over the last 82 kyr: New evidence from alkenones. *Geophys. Res. Lett.* **29**, 59-1–59-4 (2002).
122. Y. Rosenthal, D. Oppo, B.-K. Linsley, The amplitude and phasing of climate change during the last deglaciation in the Sulu Sea, western equatorial Pacific. *Geophys. Res. Lett.* **30**, 1428 (2003).
123. S. Steinke, M. Kienast, J. Groeneveld, L. C. Lin, M. T. Chen, R. Rendle-Bühring, Proxy dependence of the temporal pattern of deglacial warming in the tropical South China Sea: Toward resolving seasonality. *Quat. Sci. Rev.* **27**, 688–700 (2008).
124. L. Stott, A. Timmermann, R. Thunell, Southern hemisphere and deep-sea warming led deglacial atmospheric CO_2 rise and tropical warming. *Science* **318**, 435–438 (2007).
125. O.-C. Romero *et al.*, Orbital and suborbital variations of productivity and sea surface conditions in the Gulf of Alaska during the past 54,000 years: Impact of iron fertilization by icebergs and meltwater. *Paleoceanography & Paleoclimatology* **37** e2021PA004385 (2022).

126. M.-A. Taylor, I.-L. Hendy, D.-K. Pak., Deglacial ocean warming and marine margin retreat of the Cordilleran Ice Sheet in the North Pacific Ocean. *Earth and Planetary Science Letters* **403**, 89–98, (2014).

127. M. Yamamoto, R. Suemune, T. Oba, Equatorward shift of the subarctic boundary in the northwestern Pacific during the last deglaciation. *GRL* **32**, L05609 (2005).

128. M. Yamamoto, M. Yamamuro, Y. Tanaka, The California Current system during the last 136,000 years: response of the North Pacific High to precessional forcing. *QSR* **26**, 405-414 (2007).

129. J.-H. Velle, *et al.*, High resolution inclination records from the Gulf of Alaska, IODP Expedition 341 Sites U1418 and U1419. *Geophys. J. Int.* **229**, 345-358 (2022).

130. G. Wei, W. Deng, Y. Liu, X. Li, High-resolution sea surface temperature records derived from foraminiferal Mg/Ca ratios during the last 260 ka in the northern South China Sea. *Palaeogeogr. Palaeoclimatol. Palaeoecol.* **250**, 126–138 (2007).